

## Soundproof analysis of porous material covers for automotive parts

Yoshio Kurosawa<sup>1,a,\*</sup>, Tsuyoshi Yamashita<sup>2,b</sup>, Tetsuya Ozaki<sup>2,c</sup>,  
Naoyuki Nakaizumi<sup>2,d</sup>, Yuki Fujita<sup>2,e</sup>, and Manabu Takahashi<sup>3,f</sup>

<sup>1</sup>Faculty of Science and Technology, Teikyo University, 1-1 Toyosatodai,  
Utsunomiya City 320-8551, Japan

<sup>2</sup>Acoustic Research & Development Dept., Parker Corporation, 15 Kitane,  
Fukaya City 369-1242, Japan

<sup>3</sup>Noise Control Materials and Technology Dept., Parker Asahi Co., Ltd., 15 Kitane,  
Fukaya City 369-1242, Japan

\*Corresponding author

<sup>a</sup><ykurosawa@mps.teiyo-u.ac.jp>, <sup>b</sup><t-yamashita@parkercorp.co.jp>, <sup>c</sup><ozaki@parkercorp.co.jp>,  
<sup>d</sup><nakaizumi@parkercorp.co.jp>, <sup>e</sup><y-fujita@parkercorp.co.jp>, <sup>f</sup><takahashi-m@parker-asahi.co.jp>

**Keywords:** automotive parts, porous media, biot-allard model, fem

**Abstract.** Some automobile transmissions (AT, CVT, etc.) generate noise, and a soundproof material cover is attached to the transmission body reduce the noise by offering sound absorption and insulation. However, the sound radiating from the cover may affect the transmission of vibrations. In this study, we attached a simply shaped cover to a jig to represent a transmission body and measured the vibration acceleration and sound pressure level when the jig was vibrated. The jig and cover were modeled by FEM, and vibro–acoustic analysis was performed. The material of the cover was felt or grow wool, and sound propagation was simulated using the Biot–Allard model. This report describes the changes in vibration acceleration and sound pressure level when the method of fixing the cover and cover material are changed.

### 1. Introduction

In recent years, in-vehicle comfort has been emphasized as an aspect of automobile performance, with the quietness of the vehicle interior in great demand. Yamaguchi et al. treated a sound-absorbing double wall structure that simulates the vibration-damping and sound-insulating structure of an automobile floor as a three-dimensional problem, and analyzed its vibration damping characteristics using the finite element method [1]. Yamamoto et al. simplified an automobile body panel and passenger compartment into a rectangular flat plate and a rectangular parallelepiped sound field, and investigated a method to efficiently evaluate the effects of damping and sound absorbing and insulating materials installed at the interface on sound and vibration [2]. The authors studied for used experimental results of a simple soundproofing device and calculation results using the finite element method using a modified urethane shape in order to reduce the noise of automotive soundproofing materials that have a structure in which a rubber sheet is laminated to urethane [3].

Some automobile transmissions (such as ATs and CVTs) generate noise, which can be reduced by attaching a soundproof cover made of sound-absorbing and -insulating material. The soundproof cover is fixed to the transmission body and reduces the sound emitted from the transmission. However, the sound emitted from the soundproof cover may be affected by vibration transmission. In this study, a test piece of a soundproof cover with a simple shape was attached to an aluminum jig used to represent a transmission. The jig and soundproof cover was modeled by FEM, and vibro-acoustic analysis was performed. The material of the soundproof cover was felt or glass wool (GW), and sound propagation

was evaluated using the Biot–Allard model [1]. We will report the changes in vibration acceleration and sound pressure level when the fixing method of the soundproof cover and the material of the cover are changed.

## 2. Analytical method

The sound absorption of the felt used for the sound-absorbing duct was calculated using the Biot–Allard model [4], which handles the skeleton and internal air. In the Biot–Allard model, the incident sound entering the material is transmitted through the gaps of the porous elastic body (urethane, glass, wool, etc.) of the material, which is the air propagation sound, whereas the solid propagation sound is transmitted inside the material. This is a theoretical formula for predicting displacement. The displacement of the skeleton considering the interaction between the solid propagation and the air propagation sound:  $\vec{u}^s$  and the displacement of the fluid:  $\vec{u}^f$  are expressed as equations (1) and (2), respectively.

$$((1 - \phi) \rho_s + \rho_a) \frac{\partial^2 \vec{u}^s}{\partial t^2} - \rho_a \frac{\partial^2 \vec{u}^f}{\partial t^2} = (P - N) \vec{\nabla}(\vec{\nabla} \cdot \vec{u}^s) + Q \vec{\nabla}(\vec{\nabla} \cdot \vec{u}^f) + N \nabla^2 \vec{u}^s - \sigma \phi^2 G(\omega) \frac{\partial}{\partial t} (\vec{u}^s - \vec{u}^f) \quad (1)$$

$$(\phi \rho_f + \rho_a) \frac{\partial^2 \vec{u}^f}{\partial t^2} - \rho_a \frac{\partial^2 \vec{u}^s}{\partial t^2} = R \vec{\nabla}(\vec{\nabla} \cdot \vec{u}^f) + Q \vec{\nabla}(\vec{\nabla} \cdot \vec{u}^s) + \sigma \phi^2 G(\omega) \frac{\partial}{\partial t} (\vec{u}^s - \vec{u}^f) \quad (2)$$

$\phi$  : Porousness,  $\rho_s$  : Porous skeleton density,  $\rho_f$  : Fluid density (air in this paper),  $\rho_a$  : Equivalent density of fluid considering viscous decay in the interaction between skeleton and fluid.  $\rho_a$  is shown in Eq. (3).

$$\rho_a = \alpha_\infty \rho_f \left( 1 + \frac{\phi \sigma}{j \omega \rho_f \alpha_\infty} \sqrt{1 + j \frac{4 a_\infty^2 \eta \rho_f \omega}{\sigma^2 \Lambda^2 \phi^2}} \right) \quad (3)$$

$\eta$  : Solid loss coefficient,  $\sigma$  : Flow resistance,  $\alpha_\infty$  : Maze degree,  $\Lambda$  : Viscous characteristic length. The elastic modulus  $P, Q, R$  is shown in Eq. (4).

$$P \approx \frac{4}{3} N + K_b + \frac{(1 - \phi)^2}{\phi} K_f, \quad Q \approx (1 - \phi) K_f, \quad R \approx \phi K_f \quad (4)$$

$N$  : Skeleton shear modulus (in vacuum),  $K_b$  : Skeleton bulk modulus (in vacuum),  $K_f$  : Equivalent rigidity of fluid considering thermal decay in the interaction between skeleton and fluid.  $N, K_b, K_f$  are shown in Eq. (5).

$$N = \frac{E(1 + j\eta)}{2(1 + \nu)}, \quad K_b = \frac{2(1 + \nu)}{3(1 - 2\nu)} N, \quad K_f = \frac{\gamma P_0}{\gamma - (\gamma - 1) \left[ 1 + \frac{8\zeta}{j\omega\Lambda'^2} \sqrt{1 + \frac{j\omega\Lambda'^2}{16\zeta}} \right]^{-1}} \quad (5)$$

$\gamma$  : Specific heat ratio,  $P_0$  : Equilibrium pressure,  $\zeta$  : Thermal diffusivity,  $\Lambda'$  : Thermal characteristic length.

### 3. Experimental results and FE analysis results

#### 3.1 Comparison of the experimental results

Figure 1 shows the dimensions of the test piece and jig for the soundproof cover. The black part is a test piece made of a soundproofing material. The dimensions for the plate shape were 210 mm × 297 mm. The lower gray part is an aluminum jig, and four legs 30 mm in height were created for fixing the test piece to a plate shape extending 53 mm in the longitudinal direction of the test piece. A test piece was installed at the mounting point using one of the three fixing methods (bolts, clips, or bolts + bushings), hung using a rubber band, and vibrated at the center of the lower surface of the jig in an anechoic chamber with a hammer. The vibration response was measured with an accelerometer placed in the center. In addition, the sound pressure level during hammer vibration was measured with a microphone placed 500 mm away.

Figure 2 shows the measurements of the acceleration response and sound pressure level. The test piece this time was made of 3-mm-thick felt, and the three fixing methods (bolt fixing, clip fixing, and bolt + bush fixing) were compared. In the vibration response measurement (Fig. 2a), the bolt fixation showed the highest rigidity and the largest vibration, the clip a slightly lower vibration response, and the bush the lowest vibration response. These results may be the effect of vibration transmission reduction of the mounting method. Conversely, no significant difference was observed in the sound pressure level measurements among the three fixing methods.

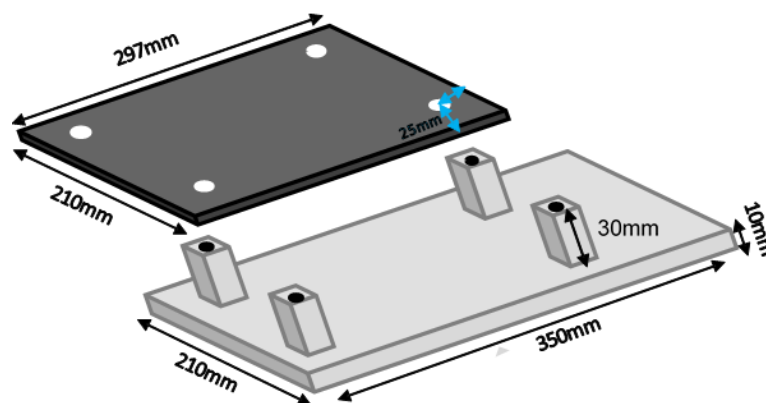


Fig. 1. Dimensions of the test piece and jig.

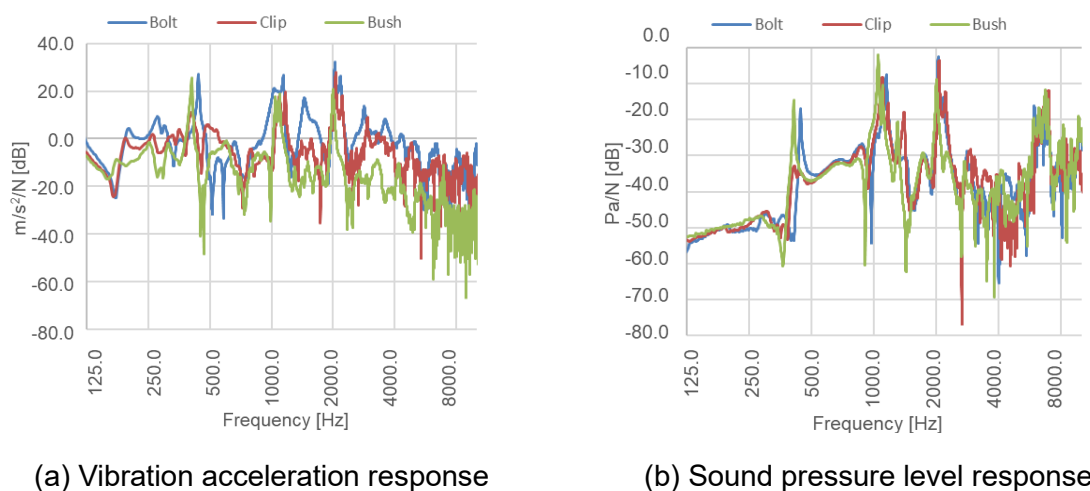


Fig. 2. Comparison of three types of mounting for each test piece.

### 3.2 Comparisons of experimental and calculated results

Figure 3 shows the FE model for the vibro-acoustic analysis. A hemispherical space was created around the hammer input point, and the spherical surface was modeled as an anechoic chamber during the experiment under non-reflecting conditions. Figures 4 to 6 show the comparison between the experimental results and the results calculated using FEM. Figure 4 shows the vibration response and sound pressure level for bolt fixing, Figure 5 the vibration response and sound pressure level for clip fixing, and Figure 6 the vibration response and sound pressure level for bush fixing. Although slight differences were found between the experimental and calculated vibration responses, the peak frequencies were approximately comparable, and the calculated results were able to reproduce the experimental results. For the sound pressure level, the calculation results also reproduced the experimental results, with a higher accuracy than the actual vibration response.

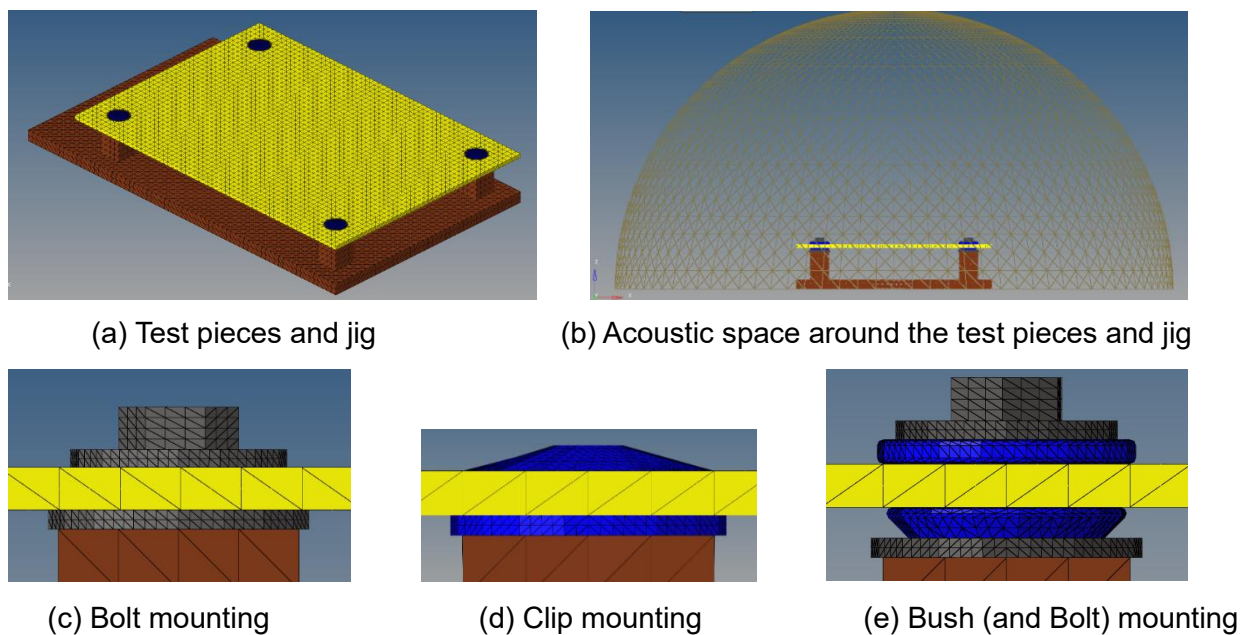


Fig. 3. FE models. In all figures, the yellow part represents the GW and the brown part represents the jig. b. represents the calculated acoustic space. In c. and d., the gray part represents the bolt, in d. the blue part represents the clip, and in e. the blue part represents the bush.

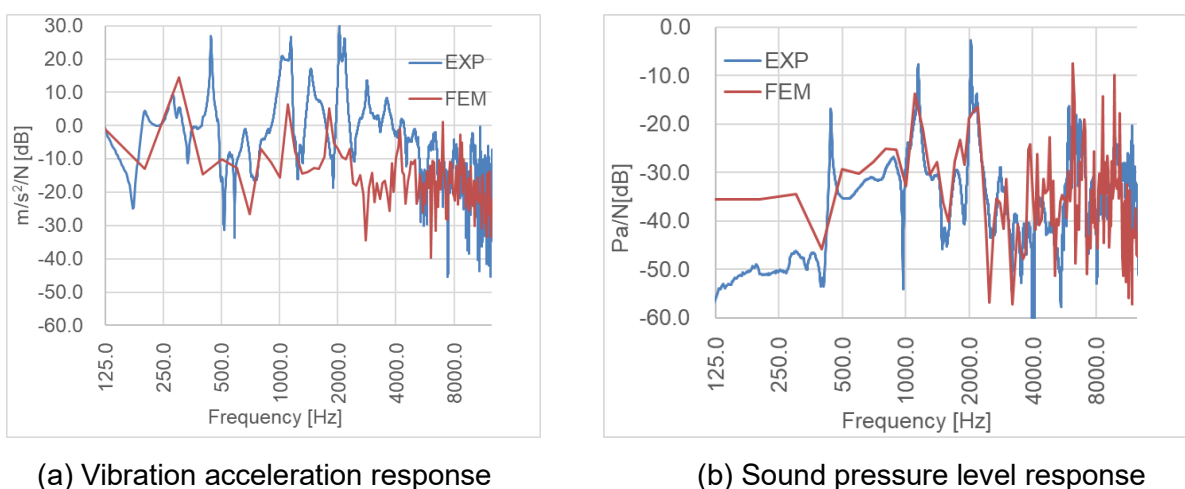
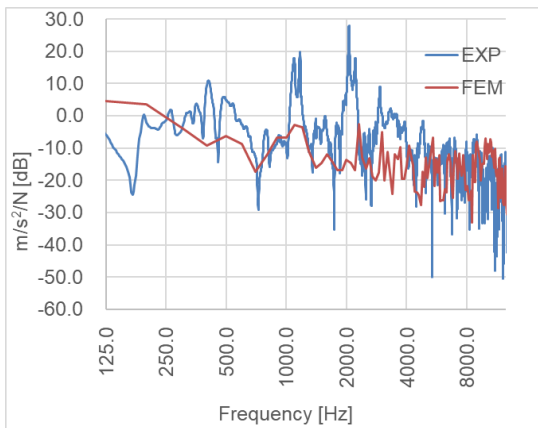
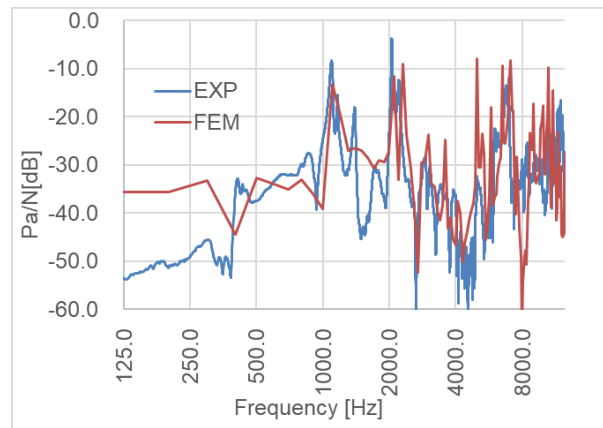


Fig. 4. Comparison of experimental results (EXP) and calculation results (FEM) by bolt mounting.

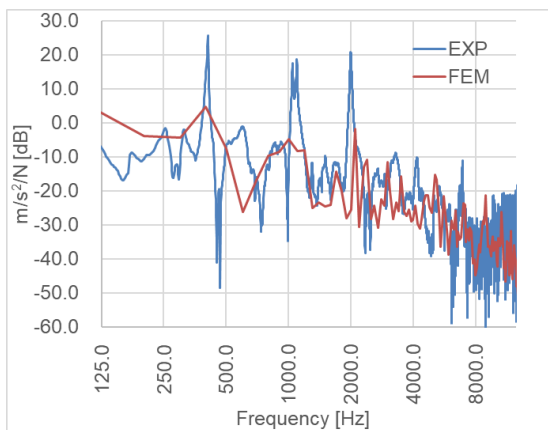


(a) Vibration acceleration response

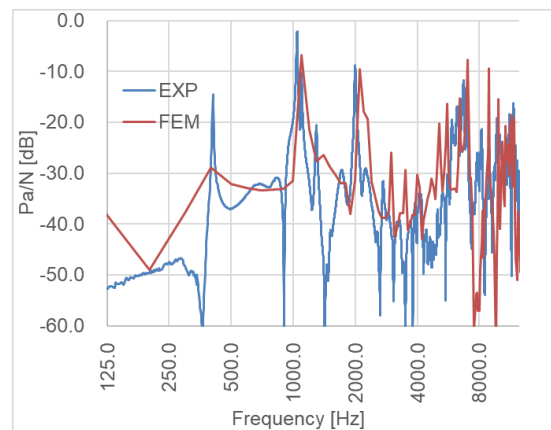


(b) Sound pressure level response

Fig. 5. Comparisons of experimental results (EXP) and calculation results (FEM) by clip mounting.



(a) Vibration acceleration response



(b) Sound pressure level response

Fig. 6. Comparison of experimental results and calculation results by bush mounting.

### 3.3 Sound insulation and sound radiation for each cover material

Based on the experimental results shown in Figure 2, the radiated sound due to the vibration of the test piece had little effect and confirmed it using the FE model. Figure 7 shows the FE model simulating the changes in acoustic space. In Figure 7a, the acoustic space is a hemisphere centered in the upper surface of the test piece. In this model, the sound radiated from the jig was not calculated. However, the vibration of the jig was transmitted to the test piece, and the radiated sound from the test piece was calculated as the sound pressure level. In addition, Figure 7b also models the space between the jig and the test piece (purple portion) as an acoustic space. The sound emitted from the test piece and that from the jig passed through the test piece. The model also calculated the sound insulation of the test piece. The difference from the initial (Figure 3a) is that the sound radiation calculated from the jig did not include the sound that went around without passing through the test piece.

Figure 8 shows a comparison of the calculated results for sound pressure level when the acoustic space is changed. The 1/3 octave band is shown for easy comparison. Figure 8a shows the calculation results for clip fixation while Figure 8b shows that for bush fixation. In clip fixation, no significant difference was found between the three fixation methods except at the 630 and 800 Hz band. However, in bush fixation, the blue line representing the radiated sound of the test piece is clearly shorter (red circle in the figure). Vibration transmission was thus reduced by the bushing, and the sound emitted from

the test piece is reduced. However, when compared with Figure 8a, almost no difference could be observed in the sound pressure level between the initials, and the effect of the sound emitted from the test piece was small. Furthermore, almost no differences were found between the values of the model with the cuboid added (orange line in the figure) and the initial (yellow line in the figure) between clip fixing and bush fixing, and the effect of the sound emitted from the jig on the test piece was small.

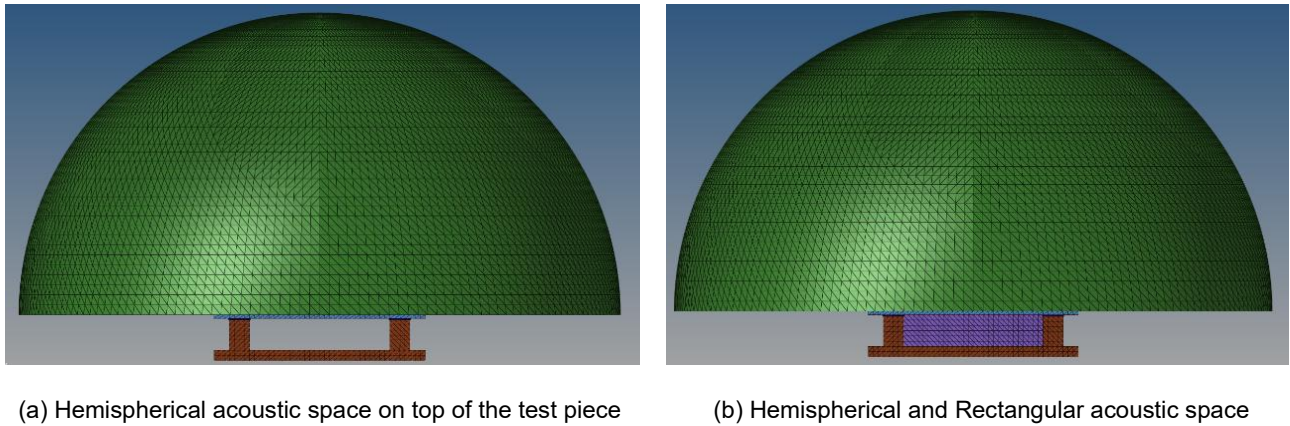


Fig. 7. FE model with modified acoustic space. In the figure, the brown part represents the jig and the green part represents the calculated acoustic space. The purple part in d represents air.

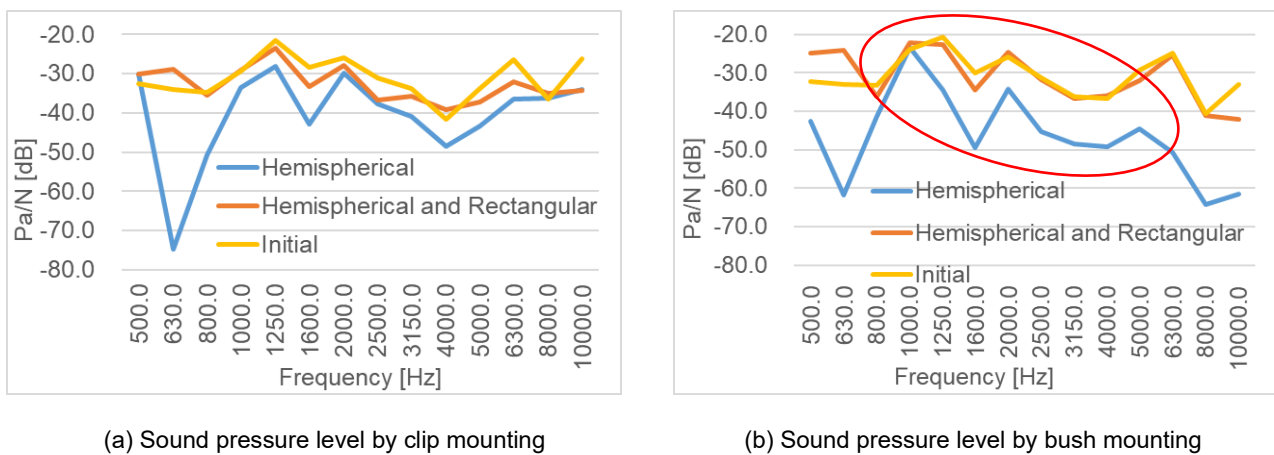
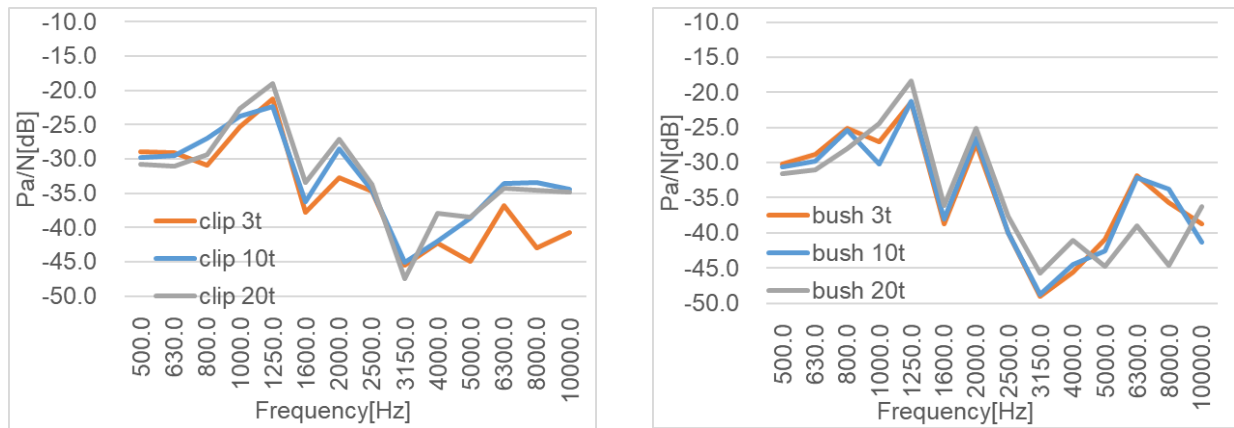


Fig. 8. Comparisons of the calculated results for sound pressure level when the acoustic space is changed.

### 3.4. Changes in thickness of the test piece

Figure 9 shows the results of calculating the sound pressure level for GW with changes in thickness for the same weight. A significant difference was found between clip fixation and bush fixation for GW.



(a) Sound pressure level by clip mounting

(b) Sound pressure level by bush mounting

Fig. 9. Comparison of GW sound pressure level calculation results with the same weight but different thickness.

#### 4. Conclusion

We created a simple model of a soundproof cover that reduced the noise from AT to measure and compare the vibration response and sound pressure level among three cover fixing methods (bolts, clips, and bushings). In vibration response, the bolt fixation showed the highest rigidity and the largest vibration, while the clip had a slightly smaller vibration response, and the bushing had the smallest vibration response. Conversely, no significant difference was found in sound pressure level among the three fixing methods. These findings indicate that the influence of the radiated sound of the soundproof cover is small. In addition, the FE model of the test piece confirmed that the sound pressure level was sufficiently accurate for analysis.

In the future, we will investigate the thickness of glass wool and study material parameters, and investigate fixing methods and material properties that will provide excellent sound performance when installed in actual automobiles.

#### References

- [1] T. Yamaguchi, H. Hozumi, Y. Kurosawa and H. Enomoto, "Damped Vibration Responses for Automotive Sound Proof Structures Using Tree-Dimensional Finite Element Method", *Transactions of the Japan Society of Mechanical Engineers*, Vol.76, No.768, pp.2016-2023, 2010.
- [2] T. Yamamoto, H. Tanaka, T. Fukushima, S. Kanehara and T. Enomoto, "An approximate method to evaluate and vibration from a thin panel covered by a damping sheet and a multi-layered soundproof structure", *Transactions of the Japan Society of Mechanical Engineers*, Vol.80, No.814, 2014.
- [3] Y. Kurosawa, T. Ozaki, N. Nakaizumi, "Sound Insulation Analysis of Automotive Soundproof Material using Urethane and Rubber", *Journal of Technology and Social Science*, Vol.2, No.1, pp.40-48, 2018.
- [4] *Propagation of sound in porous media*, J. F. Allard, N. Atalla, John Wiley & Sons (Chichester, UK), 2009.
- [5] Y. Kurosawa, J. Chengyao, T. Yamashita, T. Ozaki, N. Nakaizumi, Y. Fujita and M. Takahashi, "FE analysis of porous material covers for automotive parts", *Proceedings of Internoise2023* (Chiba, Japan), Aug 2023.